

Role of excited states for the material gain and threshold current density in quantum wire intersubband laser structures

Thomas Herrle, Stephan Haneder, and Werner Wegscheider

Institut für Experimentelle und Angewandte Physik, Universität Regensburg, 93040 Regensburg, Germany

(Received 14 February 2006; revised manuscript received 11 April 2006; published 16 May 2006)

We calculated the material gain and the threshold current density for quantum wire intersubband laser structures. In quantum cascade laser devices with active regions of lower dimensionality a reduction of the nonradiative losses and consequently an increase in the material gain and a reduction of the threshold current density is predicted. In our calculations of the material gain and the threshold current density for a realistic quantum wire intersubband laser structure fabricated by the cleaved edge overgrowth (CEO) technique, however, it turns out that excited states formed in those structures even reduce the material gain compared to conventional quantum well cascade lasers. The threshold current density also turns out to be increased due to the reduced material gain on the one hand and due to a small optical confinement factor in such structures on the other hand. The main consequence for the design of such quantum wire laser structures is to avoid the formation of excited states to be able to benefit from the reduction of the dimensionality of the electron system in terms of reduced nonradiative losses.

DOI: [10.1103/PhysRevB.73.205328](https://doi.org/10.1103/PhysRevB.73.205328)

PACS number(s): 42.55.-f, 42.55.Px, 42.60.By, 42.60.Lh

I. INTRODUCTION

In recent years quantum cascade laser structures with active regions of lower dimensionality are more and more investigated. The reason for this is the theoretical prediction of a decrease of nonradiative losses in lower dimensional systems. This is experimentally confirmed by the investigation of conventional quantum cascade lasers (QCL) in an applied magnetic field along the growth direction, where the lower dimensionality of the electron system is achieved by the Landau quantization.¹ Despite significant improvements in recent years such as room temperature continuous wave operation,² quantum cascade lasers exhibit high threshold current densities due to short nonradiative intersubband lifetimes. The use of active regions with a lower dimensionality is predicted to decrease these nonradiative losses due to a reduction of the electron-optical-phonon (LO-phonon) scattering.³⁻⁵ To this end quantum cascade structures with active regions consisting of quantum wires and quantum dots are studied theoretically as well as experimentally.⁵⁻⁹ In this work we calculate the material gain and the threshold current density for quantum wire intersubband structures. The obtained results are applied to the quantum wire intersubband structure proposed in Ref. 5. A similar device has already been realized experimentally using the cleaved edge overgrowth (CEO) technique⁶ and shows midinfrared emission at a wave number of about 1200 cm^{-1} . This device is based on the QCL structure by Sirtori *et al.* in the GaAs/Al_{0.33}Ga_{0.67}As heterosystem^{10,11} which is grown along the [001] crystal direction (x direction). However, the active region and the cladding layers are left undoped. After cleaving the heterostructure across the nonpolar (110) surface the heterostructure is overgrown in a second growth step along the [110] crystal direction (y direction). Charge carriers are supplied by a silicon modulation doping which also creates an additional confinement potential along the [110] direction. Together with the confinement potential of the quantum

wells along the [001] direction quantum wirelike states are formed at the cleavage plane with an extension of about 20 nm along the [110] direction. We compare the calculated material gain and the threshold current density of such a quantum wire laser structure with the corresponding values for the quantum cascade laser by Sirtori *et al.*¹¹

II. MATERIAL GAIN AND THRESHOLD CURRENT DENSITY IN QUANTUM WIRE LASER STRUCTURES

In order to accurately describe the electron transport and the material gain in QCL structures elaborate theoretical and numerical methods have to be applied. The relevant scattering mechanisms can be described, for example, self-consistently.¹² Wacker *et al.* use a theory based on non-equilibrium Greens functions.¹³ Iotti *et al.* perform Monte Carlo simulations to describe the electron distribution in QCL structures.¹⁴ We calculate the material gain and the threshold current density in a quantum wire cascade structure with the help of a simplified analytically solvable model, which is also used to describe conventional QCL structures.^{15,16} The optical transition rates are thereby calculated with the help of Fermi's Golden Rule and the electron transport through the structure is described by a rate equation model.

The optical transition rate from an initial state i to a final state f is given by Fermi's Golden Rule

$$W_{if} = \frac{2\pi}{\hbar} |\langle \psi_i | H' | \psi_f \rangle|^2 \delta(E_f - E_i - \hbar\omega). \quad (1)$$

ψ_i and ψ_f are the wave functions of the initial and final state of the optical transition, respectively. E_i and E_f are the corresponding energies of these states. A schematical sketch of the dispersion relations of the involved subbands is shown in Fig. 1(a). The state E_d is designed to be separated from the final state E_f by the energy of a longitudinal optical phonon

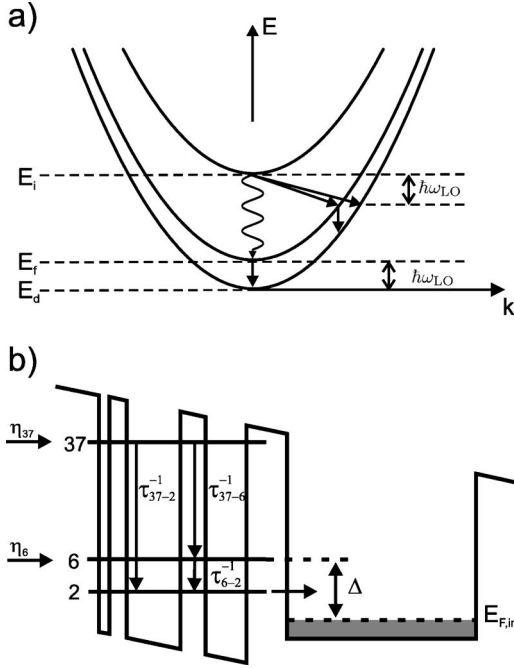


FIG. 1. (a) Schematic dispersion relation of the main subbands in a quantum wire cascade structure. The optical transition occurs between the initial state i and the final state f (wavy arrow). The final state f is depopulated by resonant longitudinal optical phonon (LO)-phonon scattering to ensure population inversion. Also depicted are some nonradiative transition processes from the initial state i . (b) Schematic diagram of the three well active region and the electron reservoir in the injector. The energetic positions of the states 37, 6, and 2 in the quantum wire cascade structure, the injection efficiencies η_{37} and η_6 and the transition rates between the states 37, 6, and 2 are shown. Transitions to excited states are not depicted for clarity.

(LO)-phonon $E_f - E_d \approx \hbar\omega_{LO}$, to ensure a fast depopulation of the final state. This provides population inversion in these structures. H' is the interaction Hamiltonian of the electron with the emitted light wave and can be written in the dipole approximation as $H' = (e/m^*)\hat{\mathbf{A}}$, with $\hat{\mathbf{A}}$ being the vector potential of the electromagnetic light wave, e the electronic charge, and m^* the effective electron mass. With the assumption of equal effective masses for the initial and final state one obtains the following expression for the transition rate

$$W_{if} = \frac{2\pi F_0^2 e^2 |\langle i | \mathbf{e} \cdot \mathbf{r} | f \rangle|^2}{\hbar} \delta(E_f - E_i - \hbar\omega). \quad (2)$$

F_0 is the modulus of the electric field, \mathbf{e} is the polarization vector of the emitted light, and $|\langle i | \mathbf{e} \cdot \mathbf{r} | f \rangle| = |\langle \psi_i | \mathbf{e} \cdot \mathbf{r} | \psi_f \rangle|$ is the matrix element of the position operator \mathbf{r} . It is noted that for conventional QCLs based on quantum wells selection rules predict transverse magnetic (TM) polarization for the emitted light. This leads to $|\langle i | \mathbf{e} \cdot \mathbf{r} | f \rangle| = |\langle i | z | f \rangle| = |z_{if}|$, where z represents the growth direction of the QCL. This means that the electric field vector of the emitted light is perpendicular to the layers of the QCL. In the quantum wire case the selection rules also allow for transverse electric (TE) polarized light. To determine the material gain of the quantum wire cascade

laser structure the net transition rate per volume V for absorption and emission of a photon between the initial and final state has to be calculated

$$R = \frac{2}{V} \sum_k (W_{em,i \rightarrow f} - W_{abs,f \rightarrow i}) [f(E_{i,k}) - f(E_{f,k})], \quad (3)$$

with the Fermi functions

$$f(E_{j,k}) = \frac{1}{\exp[(E_{j,k} - E_{F,j})/(k_B T)] + 1} \quad (4)$$

of the initial and final subbands $j=i, f$. In the quantum wire case the two quantization directions are assumed to be along the x and y direction, so that the free dispersion is along the z direction $k=k_z$. $E_{F,j}$ are the quasi-Fermi energies for the corresponding subbands. The summation in Eq. (3) is replaced by an integration

$$\frac{1}{V} \sum_k \rightarrow \frac{1}{\pi L_p L_{[110]}} \int_0^\infty dk. \quad (5)$$

The integral is normalized by two characteristic length scales of the quantum wire cascade structure. One length scale is, as in the case of a conventional QCL device, the length L_p of one period of the cascaded laser structure. The second length scale $L_{[110]}$ is the extension of the wave functions along the $[110]$ direction (y direction). In the case of the considered quantum wire cascade system $L_{[110]}$ is about 20 nm. The integral over the wave vector k can be rewritten as an integral over the energy

$$\frac{1}{\pi L_p L_{[110]}} \int_0^\infty dk \rightarrow \frac{1}{\pi L_p L_{[110]}} \sqrt{\frac{m^*}{2\hbar^2}} \int_0^\infty \frac{1}{\sqrt{E}} dE. \quad (6)$$

For the material gain in the quantum wire case $g_{1D}(\hbar\omega)$ the net transition rate R has to be divided by the photon rate per area $c \epsilon_0 n_{\text{eff}} F_0^2 / (2E_{if})$, where n_{eff} is the effective refractive index and $E_{if} = E_i - E_f$ is the energy difference between the initial and final state. With the density of states for quantum wires $D_{1D}(E) = [m^* / (2\hbar^2 \pi^2)]^{1/2} E^{-1/2}$ and the relation for the electron density $N = \int dE D_{1D}(E) f(E)$ the material gain is given by

$$g_{1D}(\hbar\omega) = \frac{e^2 E_{if} |\langle i | \mathbf{e} \cdot \mathbf{r} | f \rangle|^2}{2\hbar c \epsilon_0 n_{\text{eff}} L_p L_{[110]} (E_i - E_f - \hbar\omega)^2 + \gamma_{if}^2 / 4} (N_i - N_f). \quad (7)$$

The δ function in Eq. (2) has been replaced by a Lorentzian line shape with a full width at half maximum (FWHM) of γ_{if} . More sophisticated methods such as a density matrix formalism¹⁷ lead to a dispersive contribution to the gain profile which becomes more pronounced for decreasing population inversion.

To establish a relation between the electron densities N_i and N_f of the initial and final state, respectively, and the current density, a system of rate equations has to be set up. In the quantum wire cascade structure according to Ref. 5 the optical transition occurs between the states $i=37$ and $f=6$, which has the strongest optical transition matrix element. The final state $f=6$ is depopulated by resonant LO-phonon

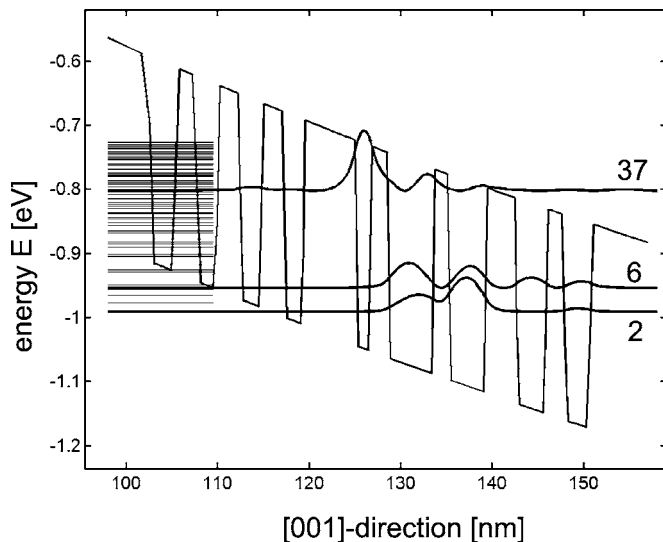


FIG. 2. Portion of the band structure cut 5 nm away from the cleavage plane together with the moduli squared of the wave functions of the states 37, 6, and 2. The lines on the left side mark the energetic positions of the first 75 wave functions. This shows that a lot of excited states are generated due to the weak confinement along the second growth direction in the quantum wire cascade structure.

scattering into state 2 with the largest LO-phonon transition rate. Because of the weak confinement potential due to the modulation doping along the [110] direction (y direction) a lot of additional states are formed, especially between the initial state $i=37$ and the lower state $f=6$ of the optical transition.⁵ In Fig. 2 the wave functions of states 37, 6, and 2 are shown together with the eigenenergies of the first 75 wave functions. Most of these states are the weakly quantized subbands of a continuum in the [110] direction of the original quantum well structure. However, the momentum space is altered for these states and scattering from the initial state $f=37$ into these states may become more probable also because of the diverging density of states in the quantum wire system as is calculated in Ref. 5. In this paper these states are referred to as excited states, since they are related to the states 6 and 2 or to states within the injector, which have single maxima at the cleavage plane. However, those excited states are energetically higher and have not only single maxima along the [110] direction at the cleavage plane but two or more maxima along this direction.⁵ The maximum with the highest probability distribution of all the maxima of the excited states lies thereby farthest away from the cleavage plane within the first growth step. In Ref. 5 it turns out that scattering from the initial state $i=37$ into state 25, which is the fourth excited state of state 6, is the most efficient scattering path, though the matrix element between these two states is quite small. However, these two states are separated energetically by about the energy of a LO-phonon. Therefore, when setting up the rate equations for a quantum wire cascade structure not only the nonradiative transitions between the states 37, 6, and 2 have to be taken into account, as is done for the corresponding states in conventional quantum well structures [see Fig. 1(b)]. Also the transitions to the

energetically lower lying excited states have to be considered. This leads to the following set of rate equations:

$$\frac{dN_{37}}{dt} = \eta_{37} \frac{J}{e} - N_{37} \sum_{l < 37} \frac{1}{\tau_{37 \rightarrow l}} - \frac{\Gamma}{N_p} \frac{c}{n_{\text{eff}}} g_{1D} N_{\text{ph}}, \quad (8)$$

$$\begin{aligned} \frac{dN_6}{dt} = & \eta_6 \frac{J}{e} + \frac{N_{37}}{\tau_{37 \rightarrow 6}} - N_6 \sum_{l < 6} \frac{1}{\tau_{6 \rightarrow l}} \\ & + N_{\text{therm}} \sum_{l < 6} \frac{1}{\tau_{6 \rightarrow l}} + \frac{\Gamma}{N_p} \frac{c}{n_{\text{eff}}} g_{1D} N_{\text{ph}}, \end{aligned} \quad (9)$$

$$\frac{dN_{\text{ph}}}{dt} = \left(\Gamma \frac{c}{n_{\text{eff}} g_{1D}} - \frac{1}{\tau_{\text{ph}}} \right) N_{\text{ph}}. \quad (10)$$

N_{37} and N_6 are the one dimensional electron densities of the corresponding states and N_{ph} is the density of photons emitted by stimulated emission. The one dimensional current density J determines the electron density per unit time being injected into the active region. The fraction $\eta_{37} J/e$ tunnels into the upper state 37 and $\eta_6 J/e$ into the lower level 6. The remaining fraction $(1 - \eta_{37} - \eta_6)$ describes electrons which tunnel directly through the optically active region into the next injector. The nonradiative transitions from state 37 and 6 to all lower lying states, including the excited states, are taken into account by the sums $\tau_{37}^{-1} = \sum_{l < 37} \frac{1}{\tau_{37 \rightarrow l}}$ and $\tau_6^{-1} = \sum_{l < 6} \frac{1}{\tau_{6 \rightarrow l}}$, which give the total lifetimes of the corresponding states τ_{37} and τ_6 , respectively. Due to the design of the energy separation between states 6 and 2 ($E_6 - E_2 \approx \hbar \omega_{\text{LO}}$) the total lifetime of state 6 is mainly given by the transition between states 6 and 2 ($\tau_6^{-1} \approx \tau_{6 \rightarrow 2}^{-1}$), because of the strong LO-phonon scattering between these two states.

The lifetime of a photon in the Fabry-Perot resonator of the considered laser structure⁹ is given by $\tau_{\text{ph}} = (\alpha_{\text{W}} + \alpha_{\text{M}})^{-1} n_{\text{eff}} / c$, with α_{W} being the waveguide losses and α_{M} the mirror losses, respectively. Electrons can be thermally activated from the electron reservoir in the injector region into the lower level 6 of the optical transition. This is referred to as thermal backfilling. This thermal activation is described by $N_{\text{therm}} = N_{\text{inj}} \exp[-\Delta / (k_{\text{B}} T)]$ with the electron density N_{inj} in the injector and the energy difference $\Delta = E_6 - E_{F, \text{inj}}$. The term $\frac{\Gamma}{N_p} \frac{c}{n_{\text{eff}}} g_{1D} N_{\text{ph}}$ represents the transition of an electron by stimulated photon emission. Further parameters are the number of periods of the cascade N_p , the optical confinement factor Γ , which is the overlap of the optical mode with the optically active region and the one dimensional material gain g_{1D} . Spontaneous photon emission is neglected in the rate equations since it is relatively weak compared to the other transitions.

In the stationary state the set of coupled differential rate equations can be solved analytically. For current densities smaller than the threshold current density ($J < J_{\text{th}}$) the electron density of state 37 is given by

$$N_{37} = \eta_{37} \tau_{37} \frac{J}{e} \quad (11)$$

and for state 6 by

$$N_6 = \tau_6 \left(\eta_6 + \eta_{37} \frac{\tau_{37}}{\tau_{37 \rightarrow 6}} \right) \frac{J}{e} + N_{\text{therm}}. \quad (12)$$

For the maximum one dimensional material gain at resonant condition ($E_{37} - E_6 = \hbar\omega$) in dependence of the current density J one obtains from Eq. (7)

$$g_{\text{max,1D}}(J) = g_{0,1D} \left(\left[\eta_{37} \tau_{37} \left(1 - \frac{\tau_6}{\tau_{37 \rightarrow 6}} \right) - \eta_6 \tau_6 \right] \frac{J}{e} - N_{\text{therm}} \right) \quad (13)$$

with

$$g_{0,1D} = \frac{2e^2 E_{37 \rightarrow 6} |\langle 37 | \mathbf{e} \cdot \mathbf{r} | 6 \rangle|^2}{\hbar c \epsilon_0 n_{\text{eff}} L_p L_{[110]} \gamma_{37 \rightarrow 6}}. \quad (14)$$

To reach threshold in quantum wire intersubband laser structures the maximum material modal gain at threshold has to overcome the waveguide and mirror losses. So the relation $\Gamma g_{\text{max,1D}}(J_{\text{th}}) = \alpha_W + \alpha_M$ has to be fulfilled which leads to a threshold current density of

$$J_{\text{th,1D}} = \left(\frac{\alpha_W + \alpha_M}{\Gamma g_{0,1D}} + N_{\text{therm}} \right) \times e \left[\eta_{37} \tau_{37} \left(1 - \frac{\tau_6}{\tau_{37 \rightarrow 6}} \right) - \eta_6 \tau_6 \right]^{-1}. \quad (15)$$

For current densities $J > J_{\text{th}}$ a constant maximum material gain of $g_{\text{max,1D}}(J > J_{\text{th}}) = (\alpha_W + \alpha_M) / \Gamma$ is assumed.

III. RESULTS AND DISCUSSION

In this section the results for the material gain and the threshold current density for a quantum wire intersubband laser structure are compared to the results for the conventional QCL structure by Sirtori *et al.*¹¹ For a comparison the thermal backfilling N_{therm} is neglected as is done for the conventional QC laser. Furthermore the injection efficiency into the upper state of the optical transition is set to unity $\eta_{37} = 1$, $\eta_6 = 0$. This leads to the following expression for the maximum material gain for quantum wire systems

$$g_{\text{max,1D}}(J) = \frac{2eE_{37 \rightarrow 6} |\langle 37 | \mathbf{e} \cdot \mathbf{r} | 6 \rangle|^2}{\hbar c \epsilon_0 n_{\text{eff}} L_p L_{[110]} \gamma_{37 \rightarrow 6}} \left[\tau_{37} \left(1 - \frac{\tau_6}{\tau_{37 \rightarrow 6}} \right) \right] J \quad (16)$$

and to an expression for the threshold current density of

$$J_{\text{th,1D}} = \frac{(\alpha_W + \alpha_M) \hbar c \epsilon_0 n_{\text{eff}} L_p L_{[110]} \gamma_{37 \rightarrow 6}}{\Gamma 2eE_{37 \rightarrow 6} |\langle 37 | \mathbf{e} \cdot \mathbf{r} | 6 \rangle|^2} \times \left[\tau_{37} \left(1 - \frac{\tau_6}{\tau_{37 \rightarrow 6}} \right) \right]^{-1}. \quad (17)$$

The assumption of a unity injection efficiency might be wrong in presence of strong elastic or inelastic scattering into the lower level of the optical transition or if the injector is not well aligned with the upper state of the optical transition.¹⁵ Furthermore, in a quantum wire cascade structure this assumption might be worse than in the quantum

TABLE I. Various parameters to evaluate the material gain and the threshold current density for a quantum well and a quantum wire cascade laser structure. The values for the quantum well structure are taken from Refs. 10 and 11, whereas the values for the considered quantum wire structure are taken from Refs. 5 and 9.

Quantum well	Quantum wire
$ z_{32} = 1.6$ nm	$ \langle 37 \mathbf{e} \cdot \mathbf{r} 6 \rangle = 1.46$ nm
$E_{32} = 134$ meV	$E_{37 \rightarrow 6} = 151$ meV
$\gamma_{32} = 15$ meV	$\gamma_{37 \rightarrow 6} = 15$ meV
$\tau_{32} = 2.40$ ps	$\tau_{37 \rightarrow 6} = 9.09$ ps
$\tau_{31} = 4.00$ ps	$\tau_{37 \rightarrow 2} = 12.5$ ps
$\tau_{21} = 0.30$ ps	$\tau_{6 \rightarrow 2} = 0.042$ ps
$\tau_3 = 1.50$ ps	$\tau_{37} = 0.91$ ps
$L_p = 45.3$ nm	$L_p = 45.3$ nm
	$L_{[110]} = 20$ nm
$n_{\text{eff}} = 3.21$	$n_{\text{eff}} = 3.25$
$\alpha_W = 20$ cm ⁻¹	$\alpha_W = 5.3$ cm ⁻¹
$\alpha_M = 21$ cm ⁻¹	$\alpha_M = 21$ cm ⁻¹
$\Gamma = 0.31$	$\Gamma = 4.3 \times 10^{-4}$

well case in view of all the excited states lying close to the upper state of the optical transition. However, this discussion stresses the importance of a close-to-unity injection efficiency in the quantum well¹⁵ as well as in the quantum wire cascade structures. Also the thermal backfilling might be different in the quantum wire case compared to the quantum well case due to the formation of excited states around the lower level of the optical transition. A nonvanishing thermal backfilling and a nonunity injection efficiency lower the maximum material gain and lead to an increased threshold current density. Therefore, the assumption of a vanishing thermal backfilling and a unity injection efficiency give an upper limit for the maximum material gain, a lower limit for the threshold current and make a comparison of the results for the quantum well and the quantum wire structures possible. The corresponding expression for the maximum material gain in the quantum well case is given by

$$g_{\text{max,2D}}(J) = \frac{2eE_{32} |z_{32}|^2}{\hbar c \epsilon_0 n_{\text{eff}} L_p \gamma_{32}} \left[\tau_3 \left(1 - \frac{\tau_{21}}{\tau_{32}} \right) \right] J, \quad (18)$$

whereas the expression for the threshold current density is given by

$$J_{\text{th,2D}} = \frac{(\alpha_W + \alpha_M) \hbar c \epsilon_0 n_{\text{eff}} L_p \gamma_{32}}{\Gamma 2eE_{32} |z_{32}|^2} \left[\tau_3 \left(1 - \frac{\tau_{21}}{\tau_{32}} \right) \right]^{-1}. \quad (19)$$

The optical transition occurs between the states 3 and 2 with the transition energy E_{32} . The level 2 is resonantly depopulated by LO-phonon scattering into level 1. The waveguide and mirror losses α_W and α_M , respectively, as well as the optical confinement factor Γ are now referred to the quantum well cascade structure. To compare the results for the quantum well and quantum wire cascade structure, the necessary parameters are given in Table I, where the values for the

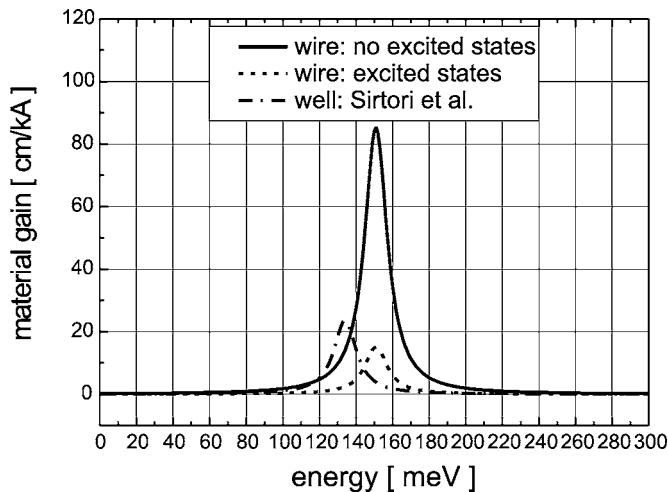


FIG. 3. Material gain for a quantum wire cascade structure according to Ref. 5 with and without considering scattering into excited states and for the quantum well cascade structure presented in Ref. 11. The material gain for the quantum wire structure is reduced compared to the quantum well system because of a reduced total lifetime of the upper state of the optical transition (see Table I). This is due to the scattering into excited states generated in the quantum wire structure. The curve where these scattering processes are neglected shows the capability to increase the material gain in quantum wire cascade structures compared to quantum well systems if the formation of excited states can be suppressed to actually increase the total lifetime of the upper state of the optical transition.

quantum well cascade structure are taken from Refs. 10 and 11 and the values for the quantum wire cascade structure from Refs. 5 and 9. In Refs. 5 and 10 LO-phonon scattering is considered to be the main scattering mechanism and thus the main source for nonradiative losses. The former reference also gives a comparison to the quantum well structure and finds results in good agreement with Refs. 10 and 11. Also Ref. 9 gives a comparison of their results to the waveguide properties of a quantum well system and also finds results in good agreement with Ref. 11. Since the FWHM $\gamma_{37 \rightarrow 6}$ of the electroluminescence shortly below threshold is not known for a quantum wire cascade laser structure we assume the same value as for the quantum well cascade structure. The mirror losses of the Fabry-Perot resonator are $\alpha_M = -\ln(R)/L$. The as-cleaved facets have a reflectivity of $R=0.27$ and the cavity length of the resonator is chosen to be $L=0.6$ mm.

To compare the material gain for the quantum well cascade structure which is given in units of [cm/kA] with the material gain in the quantum wire structure in units of [1/kA], the latter value is multiplied by the extension of the wave functions in the [110] direction of $L_{[110]}=20$ nm. The results for the material gain are shown in Fig. 3. It can be seen that the material gain in a quantum wire cascade structure is increased compared to the quantum well system if the excited states are neglected and only the states 37, 6 and 2 are taken into account when describing the scattering processes. The reason for this fact lies in the enhanced transition times $\tau_{37 \rightarrow 6}$ and $\tau_{37 \rightarrow 2}$ in the quantum wire case compared to the corresponding transition times τ_{32} and τ_{31} in the quantum

well case (see Table I). The proposed advantage of quantum wire cascade systems compared to quantum well systems actually lies in this fact. However, when the scattering to all the excited states is taken into account, the material gain of the quantum wire structure is not only reduced compared to the case when neglecting the excited states but also compared to the quantum well system. This is because of the reduced total lifetime of the upper state of the optical transition in the quantum wire case compared to the quantum well case ($\tau_{37} < \tau_3$, see Table I). Even though these excited states have a small spacial overlap with the upper state of the optical transition (state 37), the scattering rate can be quite large if the energy difference of the corresponding states is close to the LO-phonon energy.⁵ The better inversion ratio in the quantum wire case ($\tau_{37 \rightarrow 6}/\tau_6$) compared to the quantum well case (τ_{32}/τ_{21}) does not help increasing the material gain in the quantum wire case since $(1 - \tau_6/\tau_{37 \rightarrow 6})$ in the quantum wire case as well as the corresponding expression $(1 - \tau_{21}/\tau_{32})$ in the quantum well case are limited to one. Therefore the material gain is mainly determined by the total lifetime of the upper state of the optical transition and by the modulus squared of the matrix elements $|z_{32}|^2$ and $|<37|\mathbf{e} \cdot \mathbf{r}|6>|^2$ for the quantum well and quantum wire case, respectively. Some authors define a figure of merit $|z_{32}|^2 \tau_3 (1 - \tau_{21}/\tau_{32})$ for the quantum well cascade structure, which has to be maximized for a given transition energy.¹⁸ This should also be done when designing quantum cascade laser devices of lower dimensionality. In order to benefit from the advantages of lower dimensional systems the formation of excited states has to be avoided in the design of these structures. Especially LO-phonon resonances between the upper state of the optical transition and excited states have to be avoided. Calculations for quantum wire cascade structures fabricated by cleaved edge overgrowth show that this aim cannot be achieved by making changes in the second growth step alone. Efforts to redesign the first growth steps are also in progress.

Similarly the threshold current density is influenced by scattering into excited states. In Fig. 4 the maximum material gain for a quantum wire cascade laser structure as a function of the one dimensional current density is shown for the case of considering and ignoring the scattering into excited states. From the condition $g_{\max, 1D}(J_{th}) = (\alpha_W + \alpha_M)/\Gamma$ the threshold current density can be calculated. The one dimensional threshold current density when considering scattering into all excited states $J_{th, 1D} \approx 8.5$ A/cm is more than 5 times larger than without considering scattering into excited states $J_{th, 1D} \approx 1.5$ A/cm. To compare the values for the threshold current density obtained in the quantum well case $J_{th, 2D} \approx 5.7$ kA/cm² to the values obtained in the quantum wire case, these latter values are divided by $L_{[110]} = 20$ nm. This leads to a value of $J_{th, 1D} \approx 4187$ kA/cm² and $J_{th, 1D} \approx 738$ kA/cm² with and without considering scattering into excited states, respectively. The reason why the value for the threshold current density in the quantum wire case without considering scattering into excited states is almost a factor of 130 higher than in the quantum well case, lies in the fact that the optical confinement factor Γ is very much reduced in the quantum wire case compared to the quantum

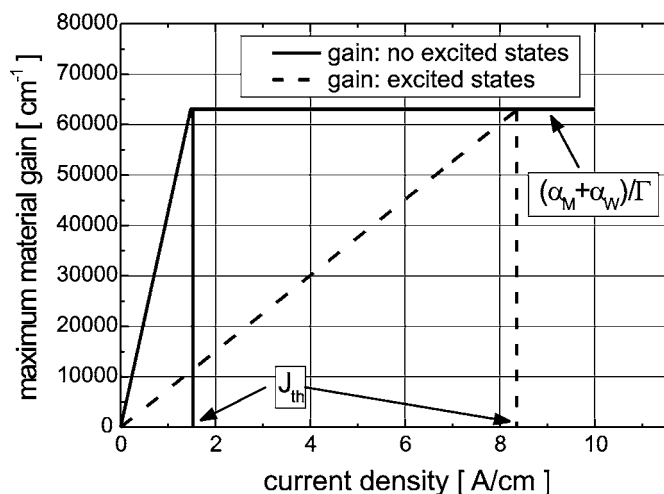


FIG. 4. Maximum material gain versus one dimensional threshold current density for a quantum wire cascade structure with and without considering scattering into excited states. From the intersection of the maximum material gain and the total waveguide losses with respect to the optical confinement factor the threshold current can be deduced. When considering scattering into excited states the threshold current turns out to be more than 5 times larger than without considering scattering into excited states.

well case (see Table I), even though the waveguide losses are reduced (see Table I) and the maximum material gain is increased (see Fig. 3). These results show that the examined quantum wire cascade structure of Ref. 5 will not work as a laser device, since the threshold current density in the GaAs/AlGaAs material system has to be lower than about 20 kA/cm^2 . In the design of quantum wire cascade devices it is therefore necessary to further decrease the total waveguide losses and more importantly to increase the confinement factor to be able to achieve laser activity. Increasing the confinement factor might be most efficient by letting several stages of coupled quantum wires overlap the optical mode instead of just one stage as in the presented structure. However, such a structure cannot be produced by CEO as in Refs. 5 and 6, but might be fabricated by self-organized lower dimensional systems like quantum wires or dots. The gain and threshold current density of the latter systems are not

discussed in this work. The absolute values for the threshold current in the quantum wire case for a sample of length $L=0.6 \text{ mm}$ are $I_{\text{th,1D}} \approx 502 \text{ mA}$ and $I_{\text{th,1D}} \approx 88.6 \text{ mA}$, with and without considering scattering into excited states, respectively. For the quantum well structure by Sirtori *et al.* with a ridge width of $30 \mu\text{m}$ and a length of $L=0.6 \text{ mm}$ a threshold current of $I_{\text{th,2D}} \approx 1.0 \text{ A}$ is calculated. For the smallest possible ridge width of about half a wavelength, which is in the case of the structure by Sirtori *et al.* about $4.5 \mu\text{m}$,¹¹ the absolute threshold current is calculated to be about $I_{\text{th,2D}} \approx 154 \text{ mA}$ for comparison. The calculated value for the threshold current density in the quantum well cascade structure is in good agreement with the results given in Ref. 11.

IV. CONCLUSION

In summary, we have calculated the material gain and the threshold current density for a quantum wire cascade laser structure with the help of Fermi's Golden Rule and with the help of a rate equation model to describe the transport through the active region. Such a model is also applied to conventional quantum well cascade lasers. It turns out that the formation of excited states in quantum wire cascade structures due to a weak confinement potential along the second growth direction decreases the total lifetime of the upper state of the optical transition. The material gain, however, is mainly determined by this lifetime and is consequently also decreased. Thus the main aim in the design of quantum wire cascade devices is to avoid the formation of excited states or at least to reduce their total number. Furthermore LO-phonon resonances between the upper state of the optical transition and excited states should be avoided. The results for the threshold current density imply that the total losses have to be further decreased and especially the optical confinement factor has to be increased to decrease the threshold current density and thus to achieve laser activity in quantum wire cascade structures.

ACKNOWLEDGMENT

This work is supported by the Deutsche Forschungsgemeinschaft within the framework of the Graduiertenkolleg "Nichtlinearität und Nichtgleichgewicht in kondensierter Materie" (GRK 638).

¹C. Becker, C. Sirtori, H. Page, A. Robertson, V. Ortiz, and X. Marcadet, Phys. Rev. B **65**, 085305 (2002).

²M. Beck, D. Hofstetter, T. Aellen, J. Faist, U. Oesterle, M. Illegems, E. Gini, and H. Melchior, Science **295**, 301 (2002).

³S. Briggs, D. Jovanovic, and J. P. Leburton, Appl. Phys. Lett. **54**, 2012 (1989).

⁴J. P. Leburton, J. Appl. Phys. **56**, 2850 (1984).

⁵I. Keck, S. Schmult, W. Wegscheider, M. Rother, and A. P. Mayer, Phys. Rev. B **67**, 125312 (2003).

⁶S. Schmult, I. Keck, T. Herrle, W. Wegscheider, M. Bichler, D. Schuh, and G. Abstreiter, Appl. Phys. Lett. **83**, 1909 (2003).

⁷N. Ulbrich, J. Bauer, G. Scarpa, R. Boy, D. Schuh, G. Abstreiter,

S. Schmult, and W. Wegscheider, Appl. Phys. Lett. **83**, 1530 (2003).

⁸S. Anders, L. Rebohle, F. F. Schrey, W. Schrenk, K. Unterrainer, and G. Strasser, Appl. Phys. Lett. **82**, 3862 (2003).

⁹T. Herrle, S. Schmult, M. Pindl, U. T. Schwarz, and W. Wegscheider, Phys. Rev. B **72**, 035316 (2005).

¹⁰Carlo Sirtori, Peter Kruck, Stefano Barbieri, Phillippe Collot, Julien Nagle, Mattias Beck, Jérôme Faist, and Ursula Oesterle, Appl. Phys. Lett. **73**, 3486 (1998).

¹¹C. Sirtori, P. Kruck, S. Barbieri, H. Page, J. Nagle, M. Beck, J. Faist, and U. Oesterle, Appl. Phys. Lett. **75**, 3911 (1999).

¹²D. Indjin, P. Harrison, R. W. Kalsall, and Z. Ikonjić, J. Appl. Phys.

- 91**, 9019 (2002).
- ¹³A. Wacker, Phys. Rev. B **66**, 085326 (2002).
- ¹⁴R. C. Iotti, and F. Rossi, Phys. Rev. Lett. **87**, 146603 (2001).
- ¹⁵J. Faist, F. Capasso, C. Sirtori, D. L. Sivco, and A. Y. Cho, *Quantum Cascade Lasers*, in *Intersubband Transitions in Quantum Wells: Physics and Device Applications II, Semiconductors and Semimetals*, edited by H. C. Liu and F. Capasso (Academic Press, New York, 2000), Vol. 62, 1–83.
- ¹⁶Q. K. Yang and A. Z. Li, J. Phys.: Condens. Matter **12**, 1907 (2000).
- ¹⁷H. Willenberg, G. H. Döhler, and J. Faist, Phys. Rev. B **67**, 085315 (2003).
- ¹⁸D. Indjin, S. Tomić, Z. Ikonić, P. Harrison, R. W. Kalsall, V. Milanović, and S. Kočinac, Appl. Phys. Lett. **81**, 2163 (2002).